



# COMPARISON OF P&O AND HILL CLIMBING MPPT ALGORITHM BASED SOLAR PV SYSTEM USING SEPIC CONVERTER

**Jalla Upendar<sup>1</sup>, Poosa Satyanarayana<sup>2</sup>, Sapavath sreenu<sup>3</sup>**

<sup>1</sup>Assistant Professor, <sup>2</sup>PG Students, <sup>3</sup>Research scholar

<sup>1,2,3</sup>Department of Electrical Engineering,

<sup>1,2,3</sup>University College of Engineering, Osmania University, Hyderabad, Telangana, India

*Abstract:* This paper present the modeling and simulation of P&O and the hill climbing (HC) algorithm for maximum power point tracking (MPPT) using Boost and SEPIC converter. This article firstly introduces a practical model of photovoltaic by which the photovoltaic array's model is obtained. The P&O and HC algorithm is used to track the maximum power from the solar panel. The MPP of solar panel varies with irradiation and temperature. The boost converter is only designed for a narrow range of line voltages, and the input current ripple is quite large. This issue is addressed by the SEPIC converters, which actually construct an LC network and add it to the BOOST converter. The entire system is implemented in MATLAB Simulink, and simulation results are displayed.

Keywords: BOOST and SEPIC Converter; P&O and Hill Climbing (HC) algorithm; Photovoltaic system.

## I. INTRODUCTION

Energy is extremely necessary for human survival, and global consumption has skyrocketed in recent years. These challenges can be resolved through research activities geared on renewable energy. Renewable energy sources (RES) have the following significant merits over traditional fossil fuel energy sources: they are supportable, never end, free, and Pollution free. RES is defined as energy derived from RES such as sun irradiation, wind, tides, and waves, among others. Solar energy is one of them, and it is growing more common in a number of applications involving heat, light, and electricity. It is especially appealing due to its quantity, renewability, hygiene, and eco-friendliness. Photovoltaic (PV) technology, which uses the PV effect to convert solar radiation directly into electricity, is one of the key solar energy technologies. PV panels undoubtedly have certain limitations, such as their minimum efficiency (9% - 17%) and susceptibility to various weather conditions [1].

Therefore, increasing conventional solar radiation is a practical strategy to raise PV panel efficiency. One of the key methods for increasing power abstraction from solar PV systems is a sun tracing system. A microprocessor was used to introduce the sun tracing systems in [2]-[7], and a programmable logic controller was used in [8]. The automatic double-axis and horizon sun tracking closed-loop control algorithms.

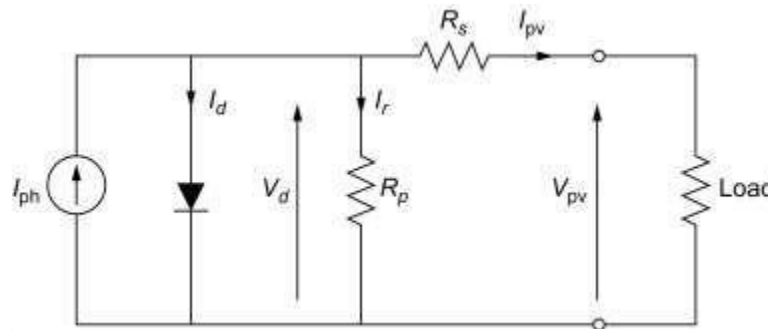
Fixed and single-axis systems were introduced and contrasted in. Additionally, it is also apparent that the solar cell's V-I characteristic is non-linear and fluctuates with temperature and irradiation [1],[9] as well as the idea made constructing and enhancing a solar tracing system. On the V-I or V-P curve, there is typically a singular point known as the MPPT. This means that the solar PV panel will operate at its best efficiency and provide the most power possible. The MPP is not known on the V-I or V-P curves, but it can be found using search techniques such as Perturbation and Observation (P&O), Artificial Neural Network (ANN), Fuzzy Logic (FL), Incremental Conductance (InC), Constant Voltage (CV), and Particle Swarm Optimization (PSO). These existing methods have many merits and demerits in terms of cost, added hardware, convergence speed, and simplicity. This study presents an enhanced InC-algorithm for monitoring an MPP on the V-I property of solar PV panels. To function in alithe and ideal set-up based on the MPPT for all conditions [10].

**II. PV SOLAR SYSTEM MODEL**

**A) Design of PV Cells:**

A p-n junction is formed in a thin layer of semiconductor material to create solar cells. To convert light energy into electrical energy, the P-N junction of a solar cell absorbs photons with energies greater than the band gap energy of the semiconductor and generates a considerable number of electron-hole pairs. The amount of radiation that photons produce current in relation to is. Several cells (usually 36 or 72) make up a PV module, which is coupled in series and parallel to produce the required output voltage and current. The commercially available technologies, the mono-crystalline technology employed in the mathematical modeling of PV cells has the highest efficiency [2]–[8]. Figure 1, displays the identical model of a solar cell circuit.

Figure 1: P-V Cell Equivalent Circuit



The equation below is a popular way to represent the physics of the PN junction diode and solar cell features, which are used to create the above circuit.

$$I_{PV} = I_{ph} - I_s \left[ e^{\frac{q(V + I \cdot R_s)}{NKT}} - 1 \right] - \frac{(V + I \cdot R_s)}{R_{sh}} \tag{1}$$

Where;

$I_{ph}$  = PV-Current

$I_s$  = Opposite saturation current of diode (A)

$q$  = Electron control ( $1.602 \times 10^{-19}$  C)

$V_{pv}$  = Voltage across the diode (V)

$K$  = Boltzmann's constant ( $1.381 \times 10^{-23}$  J/K)

$R_{se}$  = Series Resistance of the diode

$R_{sh}$  = Shunt Resistance of the diode

$N$  = Ideality factor (Ideally 1)

$T$  = Junction temperature in Kelvin (K)

**B) Characteristics of Solar cell:**

An I-V curve is used to express the output parameters of a solar cell. Figure 2, depicts a V-I curve test circuit and an example V-I curve produced by the circuit (i). To generate the V-I curve, the load resistance,  $R_L$ , is changed from 0 to infinity while current and voltage are continually measured. The juncture of the V-I curve and resistance ( $R_L$ ) marks the solar cell's operating point.  $I_p$  and  $V_p$ , respectively, represent the current and voltage at this moment. The largest working point in the square region represents the solar cell's maximum output.

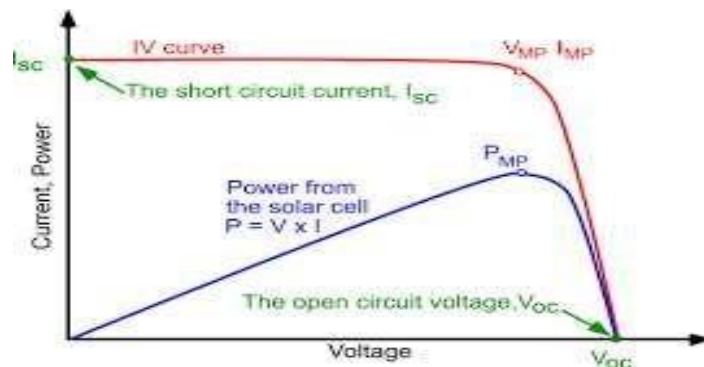


Figure 2: V-I Characteristics of Solar Cell

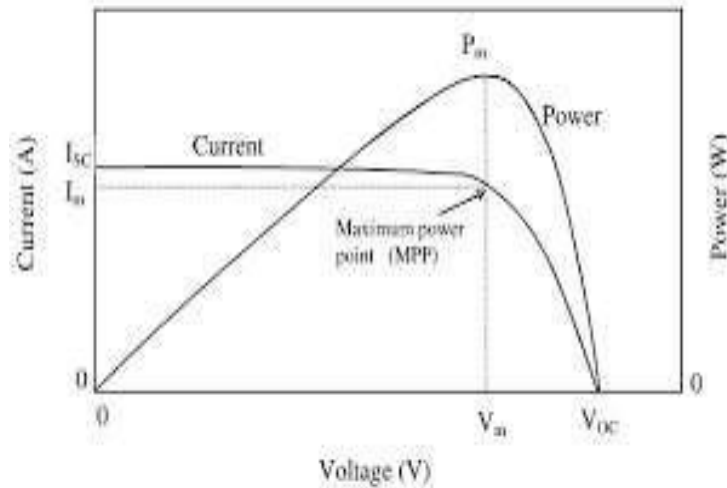


Figure 3: V-I and V-P characteristics of a solar PV panel

When the V-I characteristic and product (VI) are at their greatest levels, the solar PV cell produces the most power. Fig. 3 depicts a special point known as the MPP. Undoubtedly, the two most crucial factors to take into account when evaluating the power output of a solar PV panel are irradiance and temperature

### III. IMPLEMENTATION OF CONTROL TECHNIQUE

#### A) Perturb and Observe (P and O) :

If the power grows, more changes in that direction are considered until the power reaches a plateau. Before measuring power, the controller rapidly changes the voltage of the array. The perturb and observe method is the most used technique, despite the fact that it can lead to oscillations in power generation [15]-[16]. The power versus voltage curve must climb below the maximum power point and fall above it for the "hill rising" method to work. The most extensively utilized MPPT approach, disrupt and observe [15], is simple to implement. If an adequate predictive and adaptive hill climbing approach is used, the perturb and observe method may result in top-level efficiency.

#### B) Incremental Conductance (Inc) :

In order to predict the impacts of a voltage change, the controller use the incremental conductance technique to monitor minute variations in PV array current and voltage. Compared to the perturb and observe strategy, this method requires more work, but it can track changing conditions more quickly (P&O). It might lead to fluctuations in the power output, much as the P&O algorithm. By comparing the incremental conductance ( $I/V$ ) to the array conductance ( $I/V$ ), the maximum power point is determined using the incremental conductance approach. In the event that these two are equal ( $I/V = I/V$ ), the output voltage equals the MPP. The controller keeps this voltage until the irradiation changes, at which point the operation is repeated.

#### C) Hill climbing:

Due to its simplicity and the fact that it does not require the study or modeling of source features for age-related, shadowing, or fading quality or other operational irregularities, the hill climbing algorithm (HCA) is widely utilized. The first step is to assess the situation as it stands. The voltage ( $V(k)$ ) and current ( $I(k)$ ) of the solar cell array. The generated power ( $P(k)$ ) of the solar cell array can be estimated based on results and compared to the figure established in the previous iteration. The inscription then provides further evidence for the existence of a "slope". Depending on the slope, the PWM output is either increased or kept constant. The duty cycle changes as a result.

In photovoltaic (PV) power systems, MPPTs (maximum power point trackers) are frequently used since they optimize output power for specific parameters. These trackers' effectiveness is increased and maximized as well. As a result, an MPPT can increase maximum power production at the highest practical efficiency while lowering the overall system cost. The flow graphic fig 4, shows the Hill Climbing Algorithm [HCA] based MPPT for PV system.

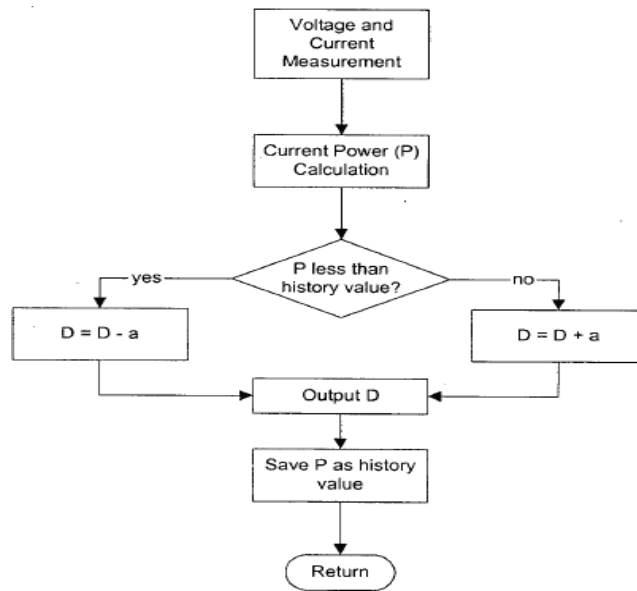


Figure 4: Hill Climbing MPPT algorithm flowchart

IV. POWER CONVERSION TOPOLOGIES

A) Boost Converter (Step-up Converter )

The fig. 5 displays the basic boost converter, this circuit is used when a higher output voltage than input voltage is required.

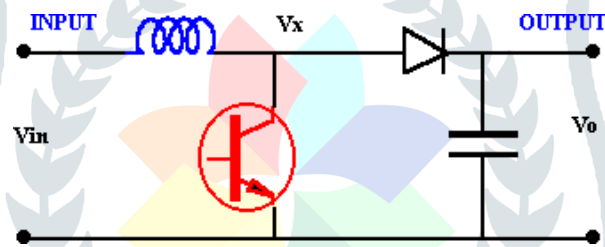


Figure 5: Boost converter circuit

When the transistor is OFF, the inductor current travels via the diode, causing  $V_x=V_o$ , and when it is ON,  $V_x =V_{in}$ . Inductor current is considered to be constant for the of this study (continuous-conduction).

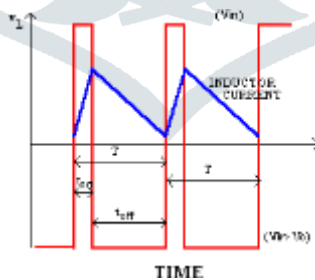


Figure 6: Boost converter voltage and current waveforms

The output voltage must always be greater in magnitude than the input voltage since the duty ratio "D" swings between 0 and 1. The negative sign indicates that the sense of the output voltage is reversed.

## B) Buck-Boost Converter

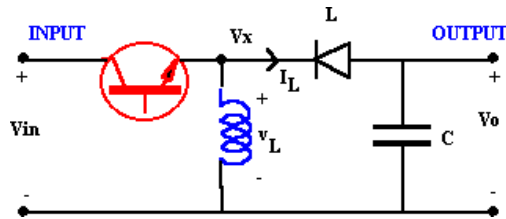


Figure 7: Schematic for a buck boost converter

In the Buck-Boost converter, continuous conduction is observed. When the transistor is turned on,  $V_x$  equals  $V_{in}$ ; when it is turned off,  $V_x$  equals  $V_o$ . When there is no change in net current over time, the inductor's average voltage is zero.

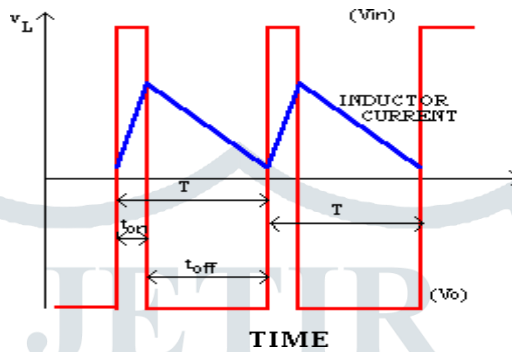


Figure 8: Waveforms for buck-boost converter

## C) Single-Ended Primary Inductor Converter (SEPIC):

The SEPIC is a type of DC/DC converter that can have an electrical potential (voltage) at its output that is either higher, lower, or equal to that at its input. The control transistor's duty cycle regulates the SEPIC's output.

Since it uses a series capacitor to couple energy from the input to the output (and as a result responds more kindly to a short-circuit output), it is similar to a conventional buck-boost converter but has the advantages of non-inverted output (the output has the same voltage polarity as the input), being able to perform true shutdown, and non-inversion of the output: The output lowers to 0 V when the switch is turned off following a significant transient charge discharge.

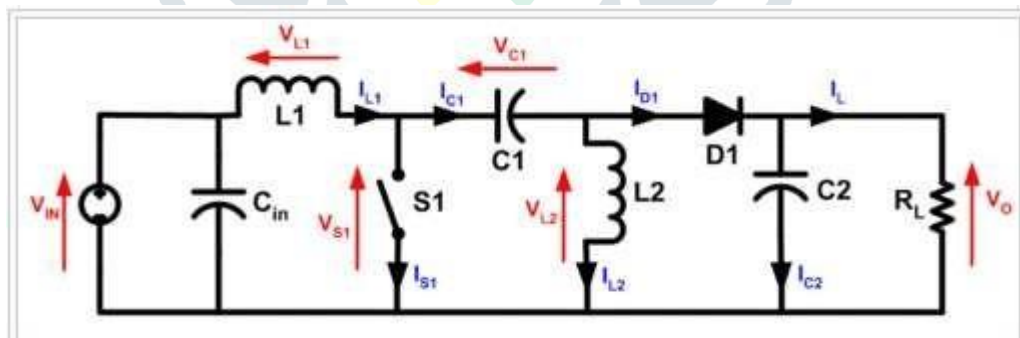


Figure 9: SEPIC's schematic diagram.

Figure 9, depicts the schematic representation of a basic SEPIC. The SEPIC converts voltage by exchanging energy between capacitors and inductors, like other switched modepower supply (more precisely, DC-to-DC converters). Determines how much energy is given through switch  $S1$ , which is often a transistor with MOSFET-like characteristics. In comparison to bipolar junction transistors, MOSFETs have a significantly higher input impedance and smaller voltage drop (BJTs). Furthermore, biasing resistors are not necessary with MOSFET switching because it is controlled by voltage differences rather than current differences, unlike BJT switching.

### i) Continuous Conduction mode:

The SEPIC is considered to be in continuous-conduction mode if the current flowing through inductor  $L1$  never hits zero (sometimes referred to as "continuous mode"). During steady-state operation, the input voltage of a SEPIC is equal to the average voltage across capacitor  $C1$  ( $V_{C1}$ ) ( $V_{in}$ ). Due to the capacitor's ability to block direct current, the average current ( $I_{C1}$ ) through capacitor  $C1$  is zero, making inductor  $L2$  the only source of the DC load current (DC). Because the average current running through the inductor  $L2$  ( $I_{L2}$ )



equals the average current flowing through the load, it is consequently voltage independent. When average voltages are taken into account, the formula below can be used.

$$V_{IN} = V_{L1} + V_{C1} + V_{L2} \tag{2}$$

The overall value of the average currents is as follows:

$$I_{D1} = I_{L1} - I_{L2} \tag{3}$$

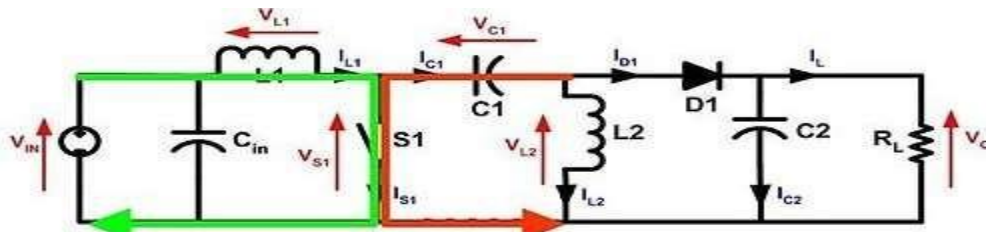


Figure10: When S1 is closed, L1 current increases.

Current  $I_{L1}$  increases and current  $I_{L2}$  decreases when switch  $S1$  is turned on. The direction of the arrow causes it to mathematically decline. The input source provides the energy needed to increase the current  $I_{L1}$ . Because  $S1$  is quickly closed, the voltage  $V_{L2}$  is close to  $V_{C1}$ , and the instantaneous voltage  $V_{L1}$  is close to  $V_{IN}$ . The capacitor  $C1$  provides the energy to increase the current in  $I_{L2}$  and, as a result, the energy held in  $L2$ . To comprehend this, see the bias voltages of the circuit in a DC state, then picture closing  $S1$  and  $C1$  increasing the current in  $L2$  of the SEPIC.

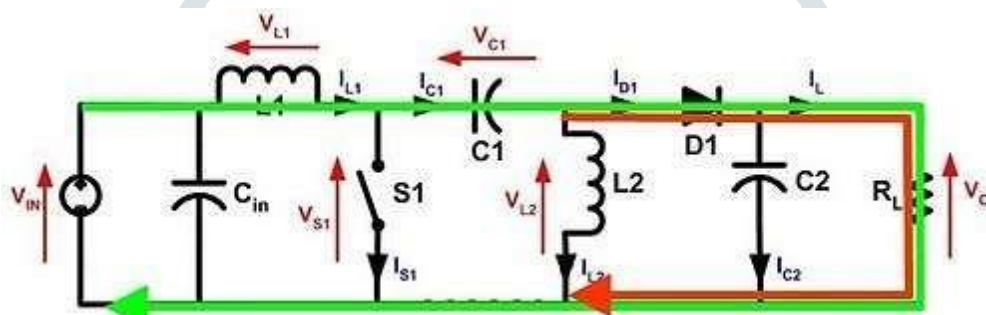


Figure 11: Current runs through L1 and L2, the SEPIC's, and S1 when it is open.

Subsequently inductors do not allow sudden changes in current; the current  $I_{C1}$  equals the current  $I_{L1}$  when switch  $S1$  is off. The present  $I_{L2}$  never changes its course and won't stop travelling in the wrong direction. The diagram depicts how increasing the amount of current delivered to the load by adding a negative  $I_{L2}$  to the existing  $I_{L1}$ . Kirchhoff's Current Law can be used to show that  $I_{D1} = I_{C1} - I_{L2}$ . Therefore, it may be deduced that power is supplied to the load from both  $L2$  and  $L1$  when  $S1$  is turned off. But during this off-cycle,  $L1$  is charging  $C1$ , and  $C1$  will then recharge  $L2$  during the on-cycle.

Because the potential (voltage) across capacitor  $C1$  may switch orientations every cycle, a non-polarized capacitor should be used. The switch must be closed for a full half cycle of resonance with inductor  $L2$  before the potential (voltage) across capacitor  $C1$  changes, and the current in inductor  $L1$  may be rather high by that time. In these cases, an electrolytic or polarized tantalum capacitor could be used.

**ii) Discontinuous Conduction mode:**

When the inductor  $L1$  current of a SEPIC is allowed to fall to zero, the device is said to be in discontinuous-conduction mode, or in this mode.

**V. MATLAB SIMULATION RESULTS**

The MATLAB/SIMULINK application is used to run simulations; Table 1: lists the program's specifications and parameters. The MPPs of the series-connected solar PV array SPR-305E-WHT-D are tracked using simulations. The maximum output power of the solar PV panel is available at an MPP with VMPP and IMPP. The MPP is established under the standard test conditions (STC) of the module temperature of 60 °C and the irradiation of 1 kW/m<sup>2</sup>. The following simulations are used to test the P&O and Hill climbing algorithms to make sure they work as planned. It differs with the hill climbing algorithms used by P&O and Hill.

Parameters	values
Maximum power ( $P_{MPP}$ )	512.4W
Voltage at $P_{mpp}$ ( $V_{MPP}$ )	54.7V
Current at $P_{mpp}$ ( $I_{MPP}$ )	5.58A
Open circuit Voltage ( $V_{oc}$ )	64.2V
Short circuit current ( $I_{sc}$ )	5.96A

Table 1: Parameters and Specifications for the Solar PV Panel SPR-305E-WHT-D

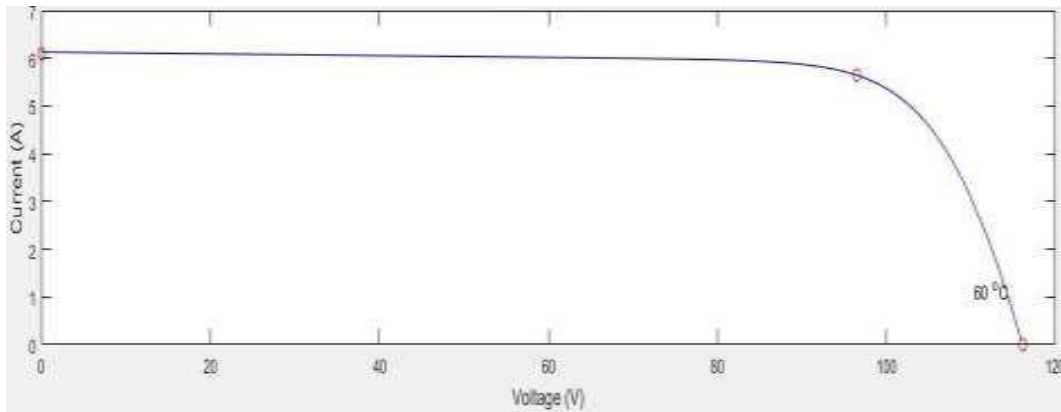


Figure 12: SPR-305E-WHT-solar D's PV panel's V-I characteristics

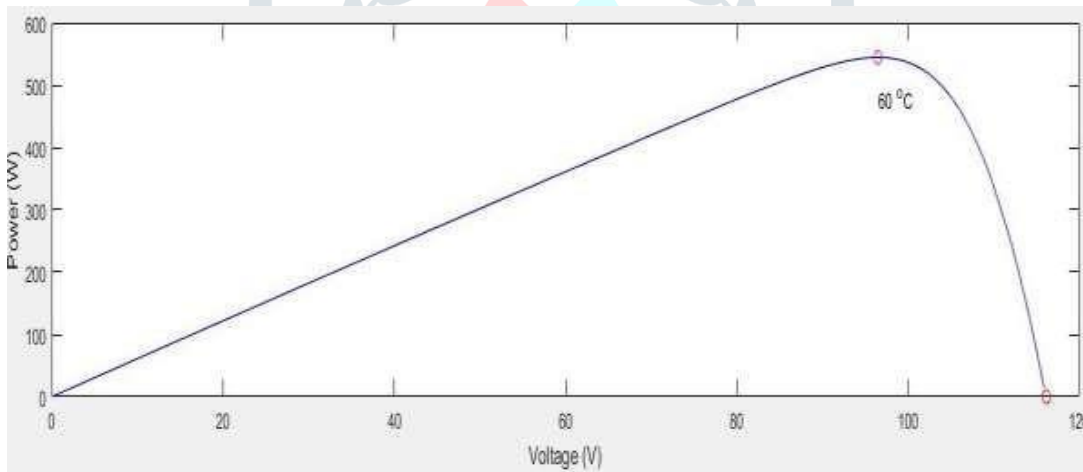


Figure13: SPR-305E-WHT-D solar PV panel's V-P characteristics

**A) P&O MPPT MODULE SIMULATION RESULTS:**

Figure 14 depicts the P&O MPPT algorithm's final modeling. Utilizing MATLAB, a thorough simulation of the final model has been performed. For  $G=1KW/m^2$  solar irradiation and  $T=60^{\circ}C$ , the simulations listed below were presented. For load  $R=40$ , simulation was run for up to 0.1 seconds.

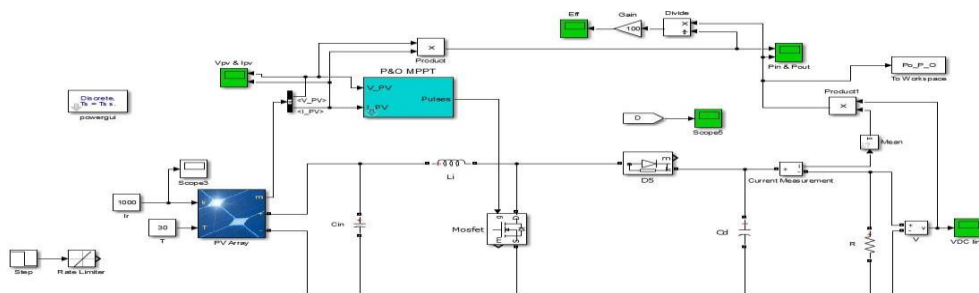


Figure 14: BOOST converter of the P&O MPPT algorithm in Simulink

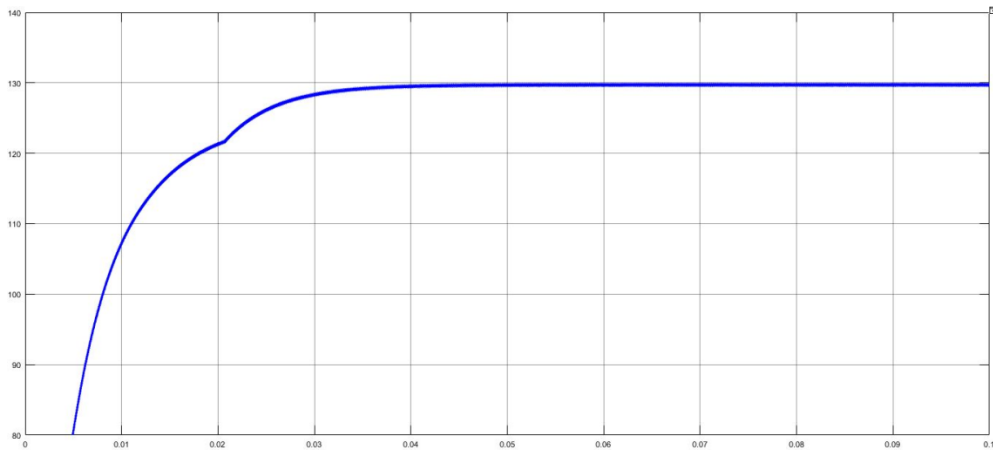


Figure 15: Output Voltage ( $V_{Out}$ ) of the BOOST converter with P&O MPPT Vs Time(sec)

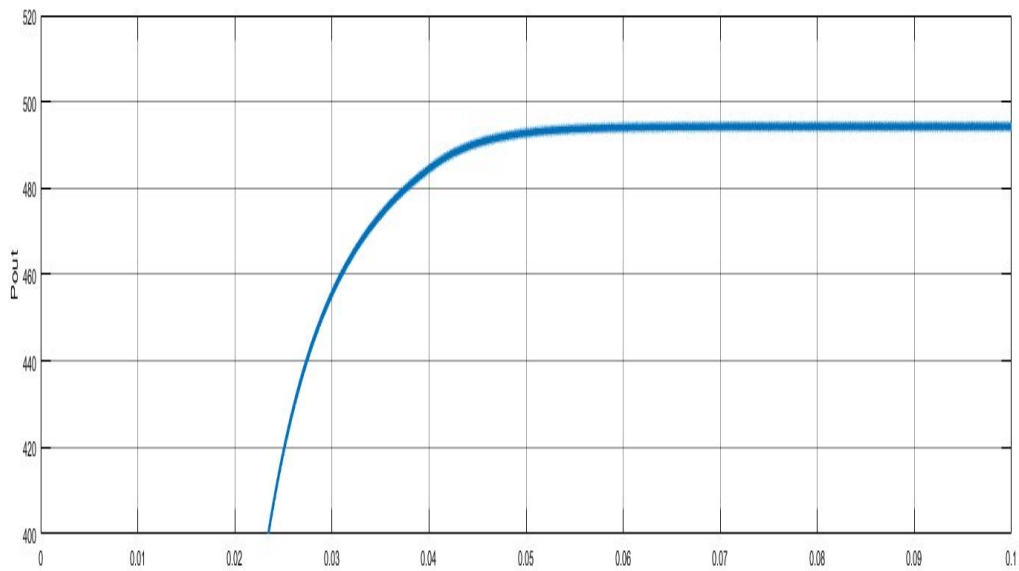


Figure 16: Output power ( $P_{Out}$ ) of the BOOST converter with P&O MPPT Vs Time(sec)

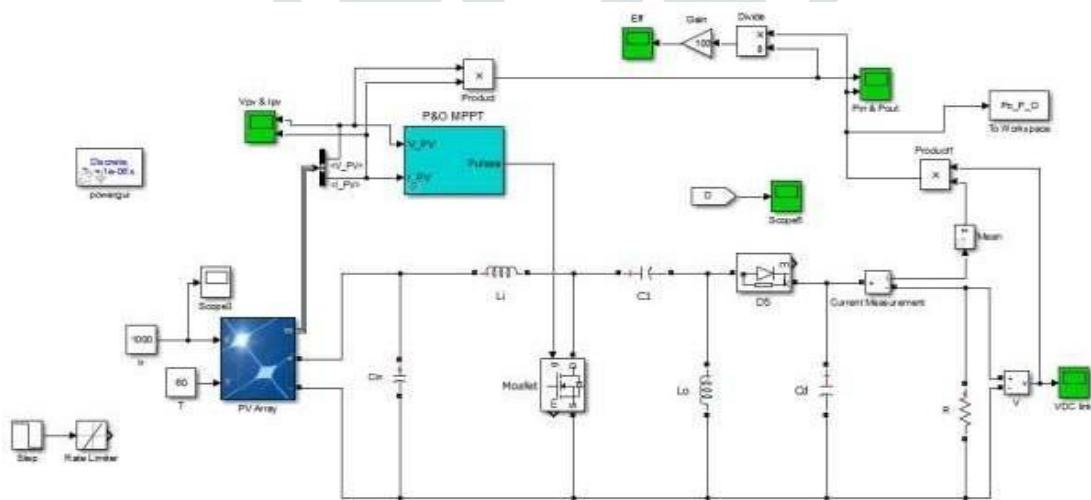
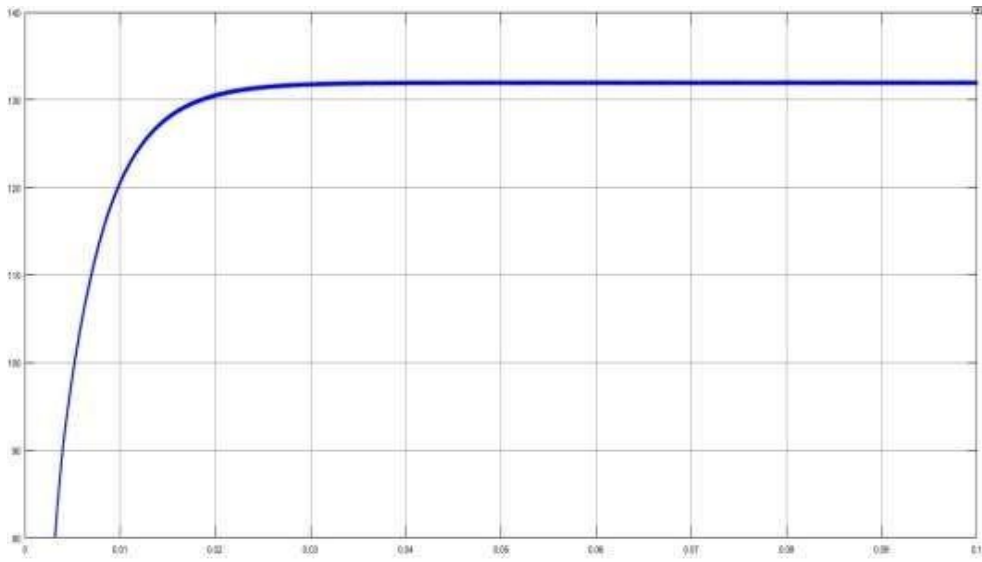
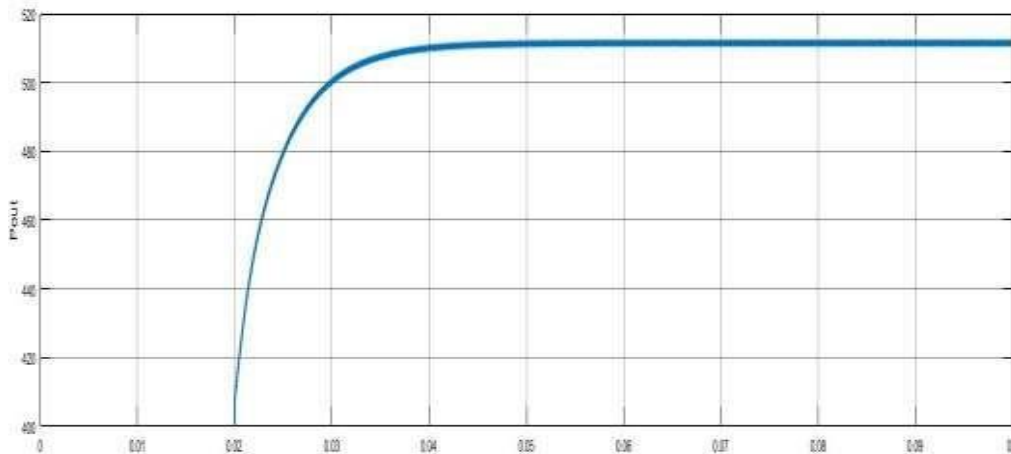


Figure 17: SEPIC converter of the P&O MPPT algorithm in Simulink



Figure 18: Output Voltage ( $V_{Out}$ ) of the SEPIC converter with P&O MPPT Vs Time(sec)Figure 19: Output power ( $P_{Out}$ ) of the SEPIC converter with P&O MPPT Vs Time(sec)

The performance of Maximum Output Power ( $P_{Out}$ ) between BOOST and SEPIC converter with P&O MPPT algorithms are given in Tables below.

Time (sec)	BOOST CONVERTER	SEPIC CONVERTER
	Output Power ( $P_{Out}$ )	Output Power ( $P_{Out}$ )
0.03	458W	500W
0.04	484W	508W
0.06	488W	510W
0.1	490W	512W

Table 2: Output Power ( $P_{Out}$ ) between BOOST and SEPIC converter with P&O MPPT algorithms

**B) HILL CLIMBING MPPT MODULE SIMULATION RESULTS:**

Figure 20: depicts the Hill Climbing MPPT algorithm's final modelling. Utilizing MATLAB, a thorough simulation of the final model has been performed. For  $G=1\text{KW}/\text{m}^2$  solar irradiation and  $T=60^\circ\text{C}$ , the simulations listed below were presented. For load  $R=40$ , simulation was run for up to 0.1 seconds.

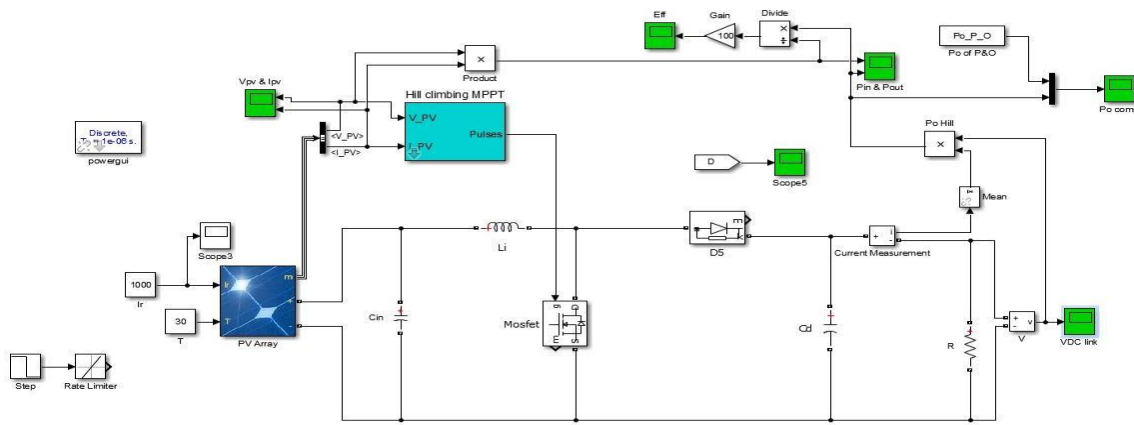


Figure 20: BOOST converter of the Hill Climbing MPPT algorithm in Simulink

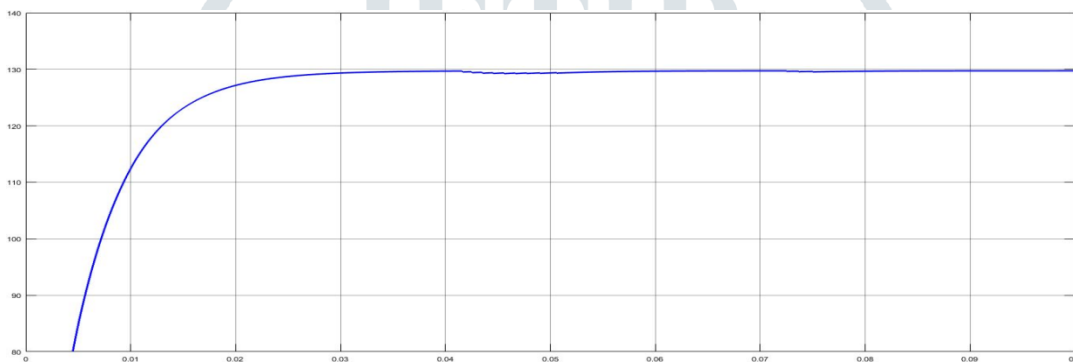


Figure 21: Output Voltage (VOut) of the BOOST converter with HC MPPT Vs Time(sec)

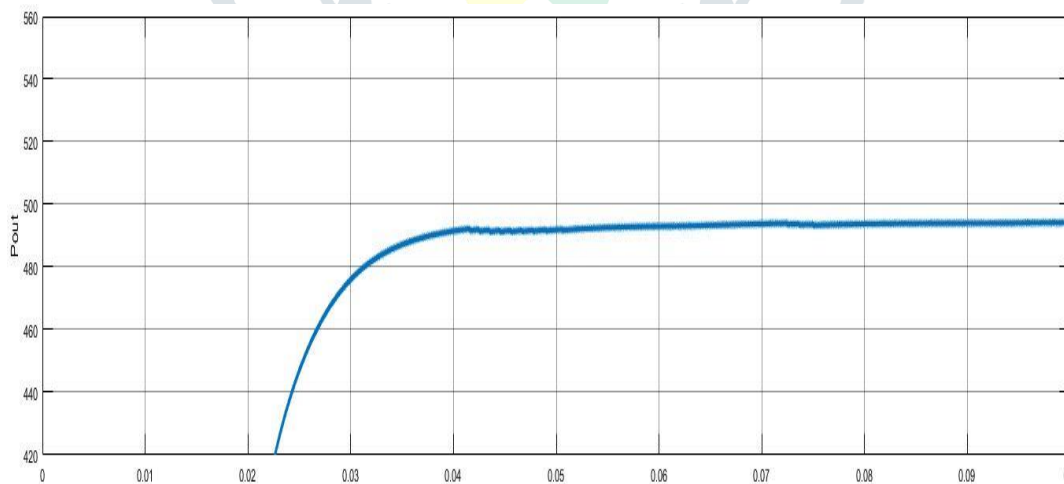


Figure 22: Output power (POut) of the BOOST converter with HC MPPT Vs Time(sec)

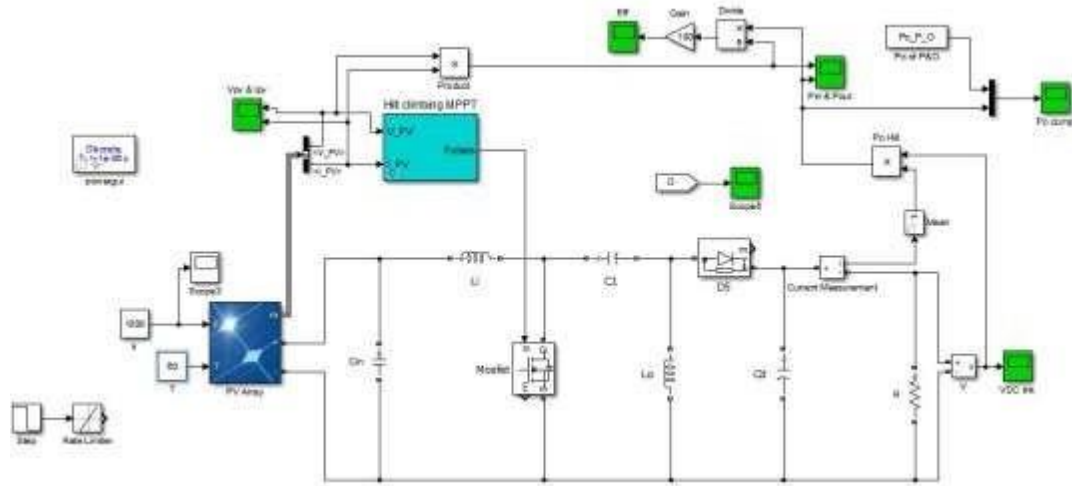


Figure 23: SEPIC converter of the HC MPPT algorithm in Simulink

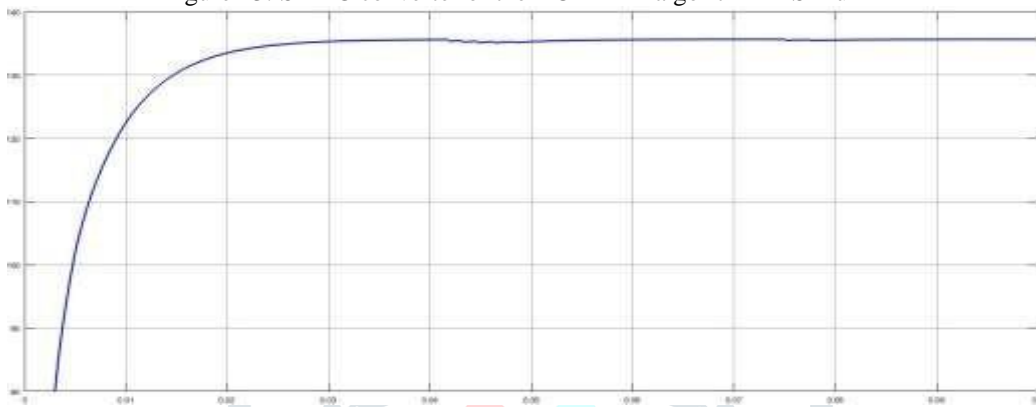


Figure 24: Output Voltage ( $V_{Out}$ ) of the SEPIC converter with HC MPPT Vs Time(sec)

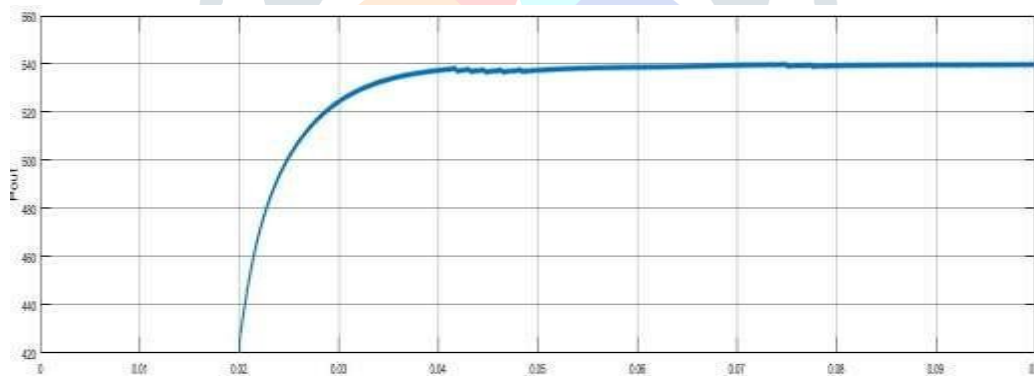


Figure 25: Output power ( $P_{Out}$ ) of the SEPIC converter with HC MPPT Vs Time(sec)

The performance of Maximum Output Power ( $P_{Out}$ ) between BOOST and SEPIC converter with P&O MPPT algorithms are given in Tables below.

Time (sec)	BOOST CONVERTER	SEPIC CONVERTER
	Output Power ( $P_{Out}$ )	Output Power ( $P_{Out}$ )
0.03	478W	522W
0.04	486W	534W
0.06	490W	540W
0.1	494W	542W

Table 3: Output Power ( $P_{Out}$ ) between BOOST and SEPIC converter with HC MPPT algorithms

**C) COMPARISON BETWEEN HILL CLIMBING and P&O MPPTs SIMULATION RESULTS:**

Figure 27: depicts the final modeling of the comparison between the Hill Climbing and P&O MPPT algorithms. Utilizing MATLAB, a thorough simulation of the final model has been performed. For  $G=1KW/m^2$  solar irradiation and  $T=60^\circ C$ , the simulations listed below were presented. For load  $R=40$ , simulation was run for up to 0.1 seconds.

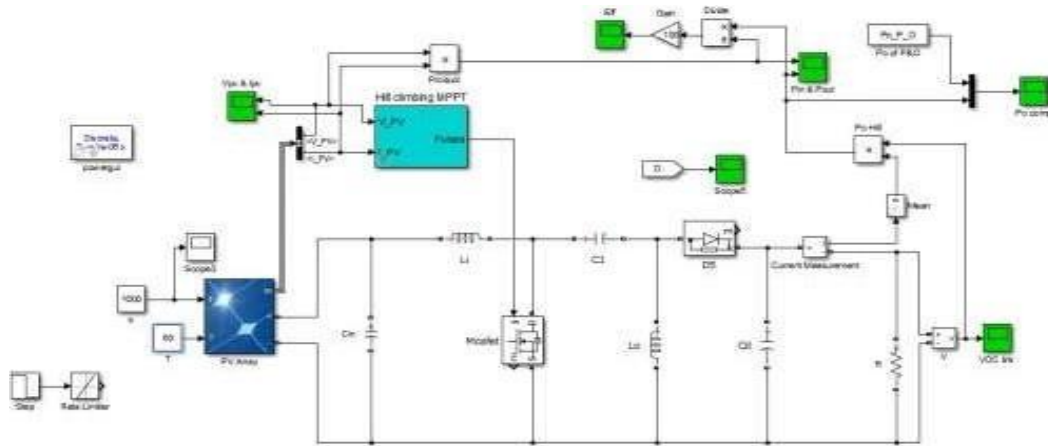


Figure 26: Simulink Model of comparison between HC and P&O MPPT-algorithm

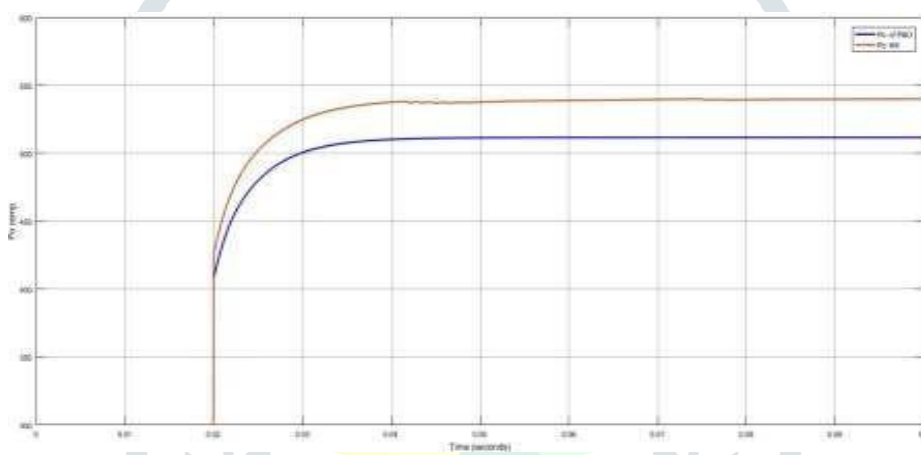


Figure 27: Comparison Output Power (POut) HC and P&O MPPTs Vs Time(sec)

The performance of Output Voltage (VOut) between P&O and HILL CLIMBING MPPT algorithms is given in Tables below.

Time (sec)	P&O MPPT	HILL CLIMBING MPPT
	Output Voltage (V <sub>Out</sub> )	Output Voltage (V <sub>Out</sub> )
0.01	120V	122V
0.02	130V	132V
0.05	132V	135V
0.1	132V	136V

Table 4: Output Voltage (V<sub>Out</sub>) between P&O and HILL CLIMBING MPPT algorithms

The performance of Maximum Output Power ( $P_{Out}$ ) between P&O and HILL CLIMBING MPPT algorithms are given in Tables below.

Time (sec)	P&O MPPT	HILL CLIMBING MPPT
	Output Power ( $P_{Out}$ )	Output Power ( $P_{Out}$ )
0.02	400W	420W
0.03	496W	524W
0.05	508W	535W
0.1	508W	540W

Table 5: Output Power ( $P_{Out}$ ) between P&O and HILL CLIMBING MPPT algorithms

## VI. CONCLUSION

We can conclude from this thesis that the input current ripple is significant and that the boost converter is only intended for a small range of line voltages. The SEPIC converters, which really build an LC network and add it to the BOOST converter, are presented as a solution to this problem. They are popular and, like the BOOST converter, do not experience casualties under stress at lower voltages. Since input current ripple in the SEPIC converter is minimal and may be directed away from input, input noise filtering is not as necessary. Consequently, SEPIC converter is better suited for solar applications than BOOST converter.

In order to obtain MPPT, the PV system with P&O and the Hill climbing algorithm has been modeled and simulated using the MATLAB/Simulink program. Both MPPT approaches' efficacy are compared and evaluated. Faster than P&O algorithm, the MPPT algorithm climbs hills to reach maximum power ( $P_{max}$ ). The suggested approach's simplicity, versatility, and quick steady-state reaction are its finest qualities. Contrasting the P&O algorithm with the Hill climbing algorithm.

## REFERENCES

- [1] Olivier CAYOL, Report avancement de project Cineli, Paris, 2013.
- [2] J.Dai and D. C. Ludois, "A Survey of Wireless Power Transfer and a Critical Comparison of Inductive and Capacitive Coupling for Small Gap Applications," *IEEE Trans. Power Electron.*, vol. 30, no. 11, pp. 6017–6029, Nov. 2015.
- [3] Sapavath Sreenu, Dr.Jalla Upendar, and Bogimi Sirisha "Analysis of Switched Impedance Source/Quasi-Impedance Source DC-DC Converters for Photovoltaic system", *International Journal of Applied Power Engineering(IJAPE)*, vol. 11, no.1, p-ISSN: 2252-8792, March-2022, doi:http://doi.org/10.11591/ijape.v11.i1.pp14-24.
- [4] Jalla Upendar, S.Ravi, Sapavath Sreenu and Bogimi Sirisha "Study and implementation of fuzzy based KY-boost converter for electric vehicle charging", *International Journal of Applied Power Engineering(IJAPE)*, vol. 11, no.1, p-ISSN: 2252-8792, March-2022, doi:http://doi.org/10.11591/ijape.v11.i1.pp98-108.
- [5] Dr.J.Upendar<sup>1</sup>, V.Aditya Yadav<sup>2</sup>, S.Sreenu<sup>3</sup>, Bogimi Sirisha<sup>4</sup> "Three-phase improved cascaded multilevel inverter with multi-carrier sinusoidal pulse width modulation with variable frequency technique for THD reduction", Published in Journal of Emerging Technologies and Innovative Research (JETIR), Issue No: 12, volume.8, Dec-2021, pp: f187-f194, ISSN:2349-5162.
- [6] S.Sreenu, Dr.N.Bhoopal and Artham Miurali "PV Based Bi-directional converter for traction application", Published in International Journal of advanced Research in electronics and communication engineering, Issue No:11, volume.6, Nov-2017, pp: 1270-1276, ISSN 2278-909X.
- [7] C. Qiu, K. T. Chau, C. Liu, and C. C. Chan, "Overview of wireless power transfer for electric vehicle charging," *Electr. Veh. Symp. Exhib. (EV27)*, 2013 World, vol.7, April 2013, pp. 1–9, 2013.
- [8] D.Jc Mac Kay, Sustainable Energy without the Hot Air, (UIT Cambridge, England,2009).
- [9] R.B.Darla, Development of maximum power point tracker for PV panel using SEPIC converter, Telecommunications Energy Conference, 2007, sept.30-oct.4.
- [10] K.Singh, A.N.Tiwari and K.P.Singh, Performance Analysis of Modified SEPIC Converter with Low Input Voltage, IJECT, Vol.3,2012,ISSUE1,ISSN: 2230-7109.
- [11] G.Walker, Evaluating MPPT converter topologies using a matlab PV model, J. Elect.Electron. Eng., Vol. 21, 2001, 45–55.
- [12] N.Femia, G. Petrone, G. Spagnuolo, and M. Vitelli, "Optimization of perturb and observe maximum power point tracking method," *IEEE Trans. Power Electron.*, vol20, no. 4, pp. 963-973, Jul. 2005.

- [13] W.Xiao, and W. G. Dunford, "A modified adaptive hill climbing mppt method for photovoltaic power systems," in *Proc. PESC*, 2004, pp. 1957-1963. Familant, Y., 2002, "A New Cascaded Multilevel H-Bridge Drive," *IEEE Trans. Power Electron.*, 17(1), pp.125-131.
- [14] H.L. Tsai, Ci-Siang Tu and Yi-Jie Su, Development of Generalized Photovoltaic Model Using Matlab/Simulink, The World Congress on Engineering and Computer Science, USA, 2008, 22-24 October.
- [15] W. DeSoto, S.A.Klein and W.A.Beckman, Improvement and Validation of a model for photovoltaic Array Performance, Elsevier Solar Energy, 2006, Vol.80, No.1, 78-88.
- [16] M. G. Villalva, J. R. Gazoli, and E. R. Filho, Comprehensive approach to modeling and simulation of photovoltaic arrays, *IEEE Trans. Power Electron*, Vol. 24, No. 5, 2009, 1198-1208.
- [17] S.Sreenu and K.R.Anugna Hindhuja "Stable power generation from PV-System Using P&O Algorithm", Published in *International Journal of Research*, Issue No:13, volume.4, Oct-2017, ISSN:2348-6848.
- [18] S.Sreenu and B.Sreenu "A Grid connected Dual voltage source inverter with power Quality improvement Features" Published in "International Journal & Magazine of Engineering Technology, Management and Research" (IJMETMR), Issue No:9, volume.3, Sept-2016, ISSN:2348-4845.
- [19] Panasonic, VBHN235SE10 specifications of photovoltaic module, data released, 2012, Mar.9.
- [20] K.Singh, A.N.Tiwari and K.P.Singh, Performance Analysis of Modified SEPIC Converter with Low Input Voltage, *IJECT*, Vol.3, 2012, ISSUE1, ISSN: 2230-7109.
- [21] M. H. Rashid, *Power Electronics Circuits Devices and Applications*, (New Jersey: Pearson Education, Inc, 3rd edition, 2004).
- [22] D.Rekious, E.Matagne, Optimization of photovoltaic Power Systems, (Springer, 2012).
- [23] M. Milosevic, On the Control of Distributed Generation in Power Systems, Thesis for the Degree of Doctor of Technical Science, Swiss Federal Institute of Technology, Switzerland, 2007.
- [24] S. A.KH.Mozaffari Niapoure, S.Danyali, M.B.B.Sharifian, M.R.Feyzi, Brushless DC Motor Drives Supplied by PV Power System Based on Z-Source Inverter and FL-IC MPPT Controller, *Energy Conversion and Management*, Vol.52, 2011, Issues 8-9, Pages 3043-3059.
- [25] T. Tafticht, K.Agbossou, M.L.Doumbia and A.Chériti, An Improved Maximum Power Point Tracking Method for Photovoltaic Systems, *Renewable Energy*, 2008, 1508- 1516.